WILEY-VCH

DOI: 10.1002/((please add manuscript number))
Article type: Communication

Polypyrenes as High-Performance Cathode Materials for Aluminum Batteries

Marc Walter,[†,‡,#] *Kostiantyn V. Kravchyk,*[†,‡,#] *Cornelia Böfer,*[†,‡] *Roland Widmer,*[£] *and Maksym V. Kovalenko*[*,†,‡]

Dr. M. Walter, Dr. K. V. Kravchyk, C. Böfer, Prof. Dr. M. V. Kovalenko

[†] Laboratory of Inorganic Chemistry, Department of Chemistry and Applied Biosciences, ETH Zürich, Vladimir-Prelog-Weg 1, CH-8093 Zürich, Switzerland
[‡] Laboratory for Thin Films and Photovoltaics, Empa – Swiss Federal Laboratories for Materials Science and Technology, Überlandstrasse 129, CH-8600 Dübendorf, Switzerland

Dr. Roland Widmer

[£] Nanotech@surfaces Laboratory, Empa – Swiss Federal Laboratories for Materials Science and Technology, Überlandstrasse 129, CH-8600 Dübendorf, Switzerland

[*]E-mail: mvkovalenko@ethz.ch
[#]Equal contributions

Keywords: Energy storage, aluminum batteries, pyrene, polypyrenes.

The pressing need for low-cost and large-scale stationary storage of electricity has led to a new wave of research on novel batteries made entirely of components that have high natural abundances and are easy to manufacture. One example of such an anode-electrolyte-cathode architecture comprises metallic aluminum, $AlCl_3$:[EMIm]Cl (1-ethyl-3-methylimidazolium chloride) ionic liquid and graphite. Various forms of synthetic and natural graphite cathodes have been tested in recent years in this context. Here, a new type of compelling cathode based on inexpensive pyrene polymers is demonstrated. During charging, the condensed aromatic rings of these polymers are oxidized, which is accompanied by the uptake of aluminum tetrachloride anions ($AlCl_4^-$) from the chloroaluminate ionic liquid. Discharge is the fast inverse process of reduction and the release of $AlCl_4^-$. The electrochemical properties of the polypyrenes can be fine-tuned by the appropriate chemical derivatization. This process is showcased here by poly(nitropyrene-co-pyrene), which has a storage capacity of 100 mAh g^{-1}, higher than the neat polypyrene (70 mAh g^{-1}) or crystalline pyrene (20 mAh g^{-1}), at a high discharge voltage (~1.7 V), energy efficiency (~86%) and cyclic stability (at least 1000 cycles).

Switching from fossil fuels to renewable, CO_2-emission-free energy sources (e.g., solar or wind power) remains a great challenge due the intermittent nature of the latter sources; consequently, large-scale energy storage solutions are needed to allow a stable energy supply and integration into the electric grid.[1, 2] Toward this goal, rechargeable battery technologies based on highly abundant metals, such as Na,[3-5] Mg,[6-11] and Al,[12-25] as charge carriers and/or electrodes have come into a major research spotlight. In particular, batteries that employ metallic Al on the anodic side harness numerous advantages, such as high natural abundance, high theoretical charge-storage capacity and high safety.[26] Unlike metallic Li or Na, Al can be safely used as an anode due to smooth, fast and dendrite-free electrodeposition in ionic liquids.[27-31] Thus, various rocking-chair-type aluminum cathodes are currently being explored in respect to the reversible insertion of Al^{3+} ions. [12-18, 20-23, 32] However, it is extremely difficult to interclate/deintercalate highly charged Al^{3+} ions in any host structure because of the high ionic charge density (Al^{3+} is even smaller than Li^{+}), which renders low ionic diffusivity and causes other difficulties such as the solvation and desolvation of ions.[33] In contrast, the facile reversible intercalation is afforded with monovalent species, such as $AlCl_4^-$. This was shown in recent publication by H. Dai group in 2015,[25] wherein porous artificial graphite can be reversibly electrochemically oxidized/reduced in $AlCl_3$:[EMIm]Cl ionic liquid (EMIm being 1-ethyl-3-methylimidazolium chloride) for thousands of cycles with concomitant intercalation/deintercalation of $AlCl_4^-$ ions within the graphene layers. In recent years, intense efforts have been devoted to unravel the structure-electrochemical property relationship for various graphites obtained synthetically[25, 34-40] or from nature,[41-47] showing charge-storage capacities of 60-150 mAh g^{-1} at average discharge voltages of 1.6-2 V.

In this work, the focus is shifted from the graphitic materials to the conjugated polymeric cathodes. Such organic electrode materials are very attractive for rechargeable batteries because they are flexible, lightweight, low-cost and safe for the environment.[48-51] Electrochemical cycling performance of conducting polymers for aluminum batteries

comprising $AlCl_3$:[EMIm]Cl ionic liquid was demonstrated only once by N. Hudak,[52] using polypyrrole and polythiophene as $AlCl_4^-$ anion-insertion cathodes. The idea that inspired this work was to emulate the cathodic behavior of the infinitely large polyaromatic graphite layers (sp^2-hybridized carbons) using only a few condensed aromatic rings. Molecular pyrene ($C_{16}H_{10}$), containing four condensed aromatic rings, was selected for this study, and the electrochemical properties of its monomeric and polymeric forms are compared herein. This choice for the organic cathodic material was motivated by the known p-type redox-activity of these materials at relatively high redox potentials, which makes them potentially useful for storage of lithium and sodium ions.[53, 54] Upon electro-oxidation, pyrene can, on average, acquire up to one positive charge per four aromatic rings to generate a radical cation, and this charge can be counterbalanced by the intercalation of $AlCl_4^-$ anions from the ionic liquid (Figure 1a). Upon electro-reduction of the polymer, the anions are released back into the ionic liquid. The corresponding theoretical charge-storage capacity is 133 mAh g^{-1} (based one electron per pyrene unit), on par with the best values for graphites. In addition, we point to the fact that intercalation of large anions, such as $AlCl_4^-$ is difficult to accomplish with conventional crystalline materials, but is a unique opportunity for materials with much greater structural flexibility such as pyrene based derivatives. Moreover, pyrene is an inexpensive material available by distillation of coal tar and is used commercially in large quantities for producing dyes and dye precursors.[55] In fact, in view of the economic efficiency of the employment of aluminum batteries for grid-scale electricity storage, it is of paramount importance to utilize low cost, earth-abundant and easy to produce components. Herein, we report that polypyrene and its derivative poly(nitropyrene-co-pyrene) can serve as highly reversible and high-capacity cathode materials for aluminum batteries, experimentally delivering capacities of 70 and 100 mAh g^{-1}, respectively, at an average voltage of 1.7 V. The poly(nitropyrene-co-pyrene) was also found to have a high cycling stability (at least 1000 cycles) at a current density of 200 mA g^{-1}.

Polypyrene was synthesized according to the oxidative polymerization procedure reported by Li *et al*.[56] (see Supporting Information, Figure S1). As shown in Figure 1b, unlike the crystalline pyrene precursor, the obtained product is almost fully amorphous. The polymerization of pyrene was further confirmed by the Fourier transform infrared (FTIR) spectra (Figure 1c). In particular, significantly lower intensities of the signals at 1184, 748 and 706 cm^{-1}, which are associated mainly with C–H deformations, and the C–H stretching vibration at 3040 cm^{-1}, indicate fewer C–H bonds as a result of the polymerization (substitution of C–H with C–C bonds).[56, 57] For the electrochemical tests, electrodes were prepared by mixing pyrene or polycyclic pyrene derivatives with carbon black (CB), polyvinylidene fluoride (PVdF) and N-methylpyrrolidone (NMP), and the resulting slurries were cast onto tungsten current collectors. A custom-made cell was employed for the electrochemical tests (Figure S2). The cell consisted of aluminum (anodic side) and tungsten (cathodic side) current collectors inside a plastic housing. Tungsten was chosen as current collector material due to its high oxidation stability (see Supporting Information, Figure S3); other common metals such as stainless steel undergo fast corrosion in $AlCl_3$-based ionic liquids. The electrodes were moderately pressed on to either side of a glass-fiber separator that was soaked with carefully dried chloroaluminate ionic liquid (mixture of [EMIm]Cl with $AlCl_3$, molar ratio: 1.3 to 1).

The working principle of the aluminum battery presented herein, as depicted in Figure 1a, can be represented by the following cathodic and anodic half-reactions during charge:

$$x Polypyrene + AlCl_4^- \rightarrow Polypyrene_x[AlCl_4] + e^- \quad (1)$$

$$4Al_2Cl_7^- + 3e^- \rightarrow Al + 7AlCl_4^- \quad (2)$$

Reaction (1) represents intercalation of $AlCl_4^-$ into polypyrene during its oxidation.[58] Reaction (2) shows electrodeposition of Al on the anode side. The charge storage mechanism proposed in Reaction (1) assumes that the only active intercalant species is $AlCl_4^-$. As follows

from X-ray photoelectron spectroscopy (XPS) measurements, intercalation of $AlCl_4^-$ ions into polypyrene was evident from the appearance of both Al 2p and Cl 2p peaks after electrochemical charging (Figure S4a, b). Additionally, energy-dispersive X-ray spectroscopy (EDX) analysis of charged polypyrene electrodes revealed the appearance of Al Kα and Cl Kα peaks (Figure S4c, d). However, taking into account that chloroaluminate ionic liquid contains a mixture of $AlCl_4^-$, $Al_2Cl_7^-$, and free Cl^- ions, intercalation of all three ions into polypyrene network during charge is possible.

Figure 2 shows the electrochemical performance of electrodes composed of pyrene and polypyrene as cathode materials in aluminum batteries at a high current density (200 mA g^{-1}). In the case of polypyrene, the capacity initially decreases, but then remains stable for 300 cycles at ~70 mAh g^{-1}, which corresponds to more than half of the theoretical value based on a one-electron redox process at the pyrene unit (133 mAh g^{-1}, see calculations of theoretical capacity in Supporting Information). Galvanostatic charge/discharge curves reveal that the storage capacity corresponds to a relatively high discharge voltage of ~1.7 V (Figure 2b). It has to be noted that electrochemical performance of polypyrene depend on the acidity of chloroaluminate ionic liquid (molar ratio of $AlCl_3$:[EMIm]Cl). As electrochemical data indicate (Figure S5), the optimal molar ratio of $AlCl_3$:[EMIm]Cl is *ca*. 1.3. In comparison to polypyrene, the performance of monomeric pyrene is quite poor. In particular, the initial discharge capacity of pyrene is only 20 mAh g^{-1} and decreases rapidly to ~10 mAh g^{-1} in subsequent cycles. Such a drastic difference in the electrochemical performance of pyrene and polypyrene can be attributed to several factors. Compared to its polymeric counterpart, pyrene not only is more prone to dissolution in the chloroaluminate ionic liquid but also is more electronically insulating due to the lack of an extended conjugated π-system. Furthermore, effective insertion of $AlCl_4^-$ is hindered by the tight packing of molecules in the crystalline pyrene. Its intermolecular distances of 3.5–4 Å[59] are too small for the diffusion of the large

$AlCl_4^-$ ions (5.3–5.9 Å).[25, 60] In contrast, an amorphous and flexible arrangement of polypyrene chains allows for diffusion of $AlCl_4^-$ ions.

To assess the impact of electron-withdrawing substituents on the electrochemical performance, a copolymer of 1-nitropyrene and pyrene was synthesized using the aforementioned synthesis procedure, but with both compounds as starting materials in a 1:1 molar ratio. The resulting product was amorphous (Figure S6) and shows almost the same FTIR-spectrum as polypyrene with the main difference being additional vibrations at 1510 cm^{-1} and 1330 cm^{-1} (Figure 3a). These additional vibrations can be attributed to the vibrations of NO_2-groups, specifically the N=O asymmetric stretches (typically found at 1660-1490 cm^{-1}) and N=O symmetric stretches (typically found at 1390-1260 cm^{-1})[61] (see also Figure S7), which indicates the successful formation of a copolymer of pyrene and 1-nitropyrene.

C, H, and N elemental analysis suggested an atomic ratio C:N of 45:1, corresponding to approximately three pyrene per NO_2-group. Hence, the number of nitropyrene units in the poly(nitropyrene-co-pyrene) is lower than one would expect based on a 1:1 mixing ratio of monomers before polymerization. Regarding molecular weight determination, it should be noted that much like polypyrene,[56] the poly(nitropyrene-co-pyrene) is poorly soluble in common organic solvents. Gel permeation chromatography (GPC) with tetrahydrofuran (THF) as the eluent revealed that in the case of both polypyrene and poly(nitropyrene-co-pyrene), the soluble fraction contains mostly oligomeric species with fewer than 10 repeating units (Figure S8).

Figures 3b-d summarize the results of the electrochemical tests with poly(nitropyrene-co-pyrene) as the cathode material in aluminum batteries carried out at a current density of 200 mA g^{-1} and in the potential range of 1.05–2.2 V. Similar to polypyrene, almost no capacity fading was observed for 100 cycles with a stable average discharge voltage of ~1.7 V. Relatively high coulombic efficiencies (~97%) and energy efficiencies (86%) were obtained. Furthermore, even at a high charging/discharging rate (2000 mA g^{-1}) poly(nitropyrene-co-

pyrene) shows minimal capacity fading after 500 cycles with an average capacity of ~48 mAh g^{-1} (Figure S9). Interestingly, the poly(nitropyrene-co-pyrene) shows significantly higher capacities than the polypyrene sample, yet the profile of the galvanostatic charge and discharge curves remains almost the same (Figure 3c), indicating that the introduction of NO_2-groups is likely not significant for the redox potential. Plausible explanations for the higher observed capacity are that the poly(nitropyrene-co-pyrene) shows better dispersibility in NMP than the homopolymer and is therefore in potentially better contact with the conductive additive (CB) or that there are structural differences between the homopolymer and copolymer (e.g., spacing between the polymer chains, porosity, etc.) that lead to utilization of a higher fraction of the active material. However, it should be noted that much poorer battery performance was observed for materials obtained by polymerization of only 1-nitropyrene (Figure S10). Thus far, the only reported work on polymers as cathodes for aluminum batteries utilizes polythiophene and polypyrrole,[52] and identical cells with Al and $AlCl_3$:EMIMCl were assembled. However, these polymers showed lower discharge voltages and worse cyclabilities and rate capabilities than poly(nitropyrene-co-pyrene) (see Table S1 for detailed comparison).

The electrochemical performances of polycyclic pyrene derivatives are on par with the performances of graphitic materials, which exhibit capacities of 60-150 mAh g^{-1} and average discharge voltages of 1.6-2.0 V, exemplifying the great utility of polymeric materials and in particular copolymers for aluminum batteries. The unique features of polycyclic aromatic polymers, such as their low cost, lightweight, flexibility and solution processability,[55, 62] might offer new opportunities in low-cost battery technologies.

In summary, we have demonstrated a proof-of-concept for aluminum batteries with inexpensive pyrene-based polymers as high-performance cathode materials. Whereas crystalline monomeric pyrene shows insignificant charge-storage capacities, good electrochemical performances were obtained with amorphous polypyrene, which could be

further improved by using a copolymer of pyrene and nitropyrene. In particular, stable cycling with an average capacity of 100 mAh g^{-1} and a discharge voltage of 1.7 V for 1000 cycles at a current density of 200 mA g^{-1} was demonstrated for poly(nitropyrene-co-pyrene) with high coulombic efficiency (97-98%) and energy efficiency (86%). We note that that prior to practical application of this class of materials substantial further work is needed, particularly on understanding the atomistic details of charge storage and fading mechanisms, as well as optimization of the electrode mass-loading for obtaining practically relevant areal capacities. Considering the vast possibilities of polymeric aromatic hydrocarbon compounds, specifically in terms of compositional and structural tunability, low cost, high abundance and production scalability, this work provides further inspiration for the development of rechargeable aluminum batteries.

Experimental Section

Polymeric cathode materials. Polypyrene was synthesized and purified according to the procedure reported by Li et al.[56] To synthesize poly(nitropyrene-co-pyrene), the same procedure was used with pyrene and 1-nitropyrene as starting materials in a 1:1 molar ratio. The resulting materials were further purified with acetonitrile and chloroform to completely remove unreacted 1-nitropyrene.

Electrode fabrication, cell assembly, and electrochemical measurements. The following battery components were used: carbon black (Super C65, TIMCAL), poly(vinylidene fluoride) (PVdF, Sigma-Aldrich), N-methyl-2-pyrrolidone (NMP, 99%, Sigma-Aldrich), anhydrous $AlCl_3$ (99.99%, ABCR), 1-ethyl-3-methylimidazolium chloride ([EMIm]Cl, 99%, ABCR; dried at 130 °C under vacuum), and glass microfiber separator (GF/D, Whatman). Electrodes were prepared by mixing the active material with PVdF and NMP using a Fritsch Pulverisette 7 classic planetary mill with zirconia beaker and 50 zirconia balls (5 mm in

diameter) for 1 hour at 500 rpm. The composition of the slurry was 50% pyrene-based polymer, 40% CB and 10% PVdF. This fraction of CB was used to provide sufficiently high electrode conductivity. Slurries were coated onto tungsten current collectors (Alfa Aesar) and were dried at 80 °C for 12 hours under vacuum (with loading of active material ~ 0.5 mg cm^{-2}). For measurements with pyrene, slurries were prepared using cyclopentanone instead of NMP as a solvent, and the current collectors were dried at room temperature for 12 hours under vacuum. Electrochemical measurements were conducted in homemade, reusable, air-tight cells assembled in an Ar-filled glove box (O_2 < 0.1 ppm, H_2O < 0.1 ppm) using 60 μL of $AlCl_3$-[EMIm]Cl ionic liquid per cell. Aluminum foil (thickness: 11 μm) was used as both the reference and counter electrode. $AlCl_3$-[EMIm]Cl ionic liquid was prepared by slowly mixing the EMIMCl and $AlCl_3$ powders in an argon-filled glove box. Afterwards, the ionic liquid was treated with Al foil at 150 °C for 6 h. A piece of glass fiber was used as the separator and dried overnight at 120°C under vacuum prior to use. Galvanostatic cycling tests were carried out at room temperature with an MPG2 multi-channel workstation (BioLogic). Capacities were normalized by the mass of the respective pyrene-based polymer.

Materials characterization. Powder X-ray diffraction (XRD) was performed with a STOE STADI P powder X-ray diffractometer (Cu-Kα_1 irradiation, λ = 1.540598 Å). Scanning electron microscopy (SEM) measurements were collected using a NanoSEM 230. Attenuated total reflectance Fourier transform infrared (ATR-FTIR) spectroscopy measurements were collected on a Nicolet iS5 FT-IR spectrometer (Thermo Scientific). Gel permeation chromatography was carried out using an Agilent GPC 1100 with tetrahydrofuran as the eluent. C, H, and N elemental analysis was carried out using a LECO TruSpec Micro. X-ray photoelectron spectroscopy (XPS) measurements were carried out in normal emission using a monochromatized Al Kα X-ray radiation source and a Scienta R3000 display analyzer. Energy-dispersive Energy-dispersive X-ray spectroscopy (EDX) measurements were carried

out using an EDAX Octane Super spectrometer (Ametek) attached to a Quanta 200F scanning electron microscope (Thermo Fisher Scientific).

Supporting Information
Supporting Information is available from the Wiley Online Library or from the author.

Acknowledgements
This work was financially supported by ETH Zürich (Grant Nr. ETH-56 12-2), the Swiss Federal Commission for Technology and Innovation (CTI-Project Nr. 14698.2 PFIW-IW) and CTI Swiss Competence Centers for Energy Research (SCCER Heat and Electricity Storage). The authors thank Beatrice Fischer and Prof. Dr. Frank Nüesch for GPC measurements and the micro-laboratory at ETH Zürich for CHN analysis. The authors thank Dr. Frank Krumeich for EDX measurements. Electron microscopy was carried out at the Empa Electron Microscopy Center.

Received: ((will be filled in by the editorial staff))
Revised: ((will be filled in by the editorial staff))
Published online: ((will be filled in by the editorial staff))

References

[1] R. Van Noorden, *Nature* **2014**, *507*, 26.

[2] D. Larcher, J. M. Tarascon, *Nat. Chem.* **2015**, *7*, 19.

[3] H. Pan, Y.-S. Hu, L. Chen, *Energy Environ. Sci.* **2013**, *6*, 2338.

[4] M. D. Slater, D. Kim, E. Lee, C. S. Johnson, *Adv. Funct. Mater.* **2013**, *23*, 947.

[5] V. Palomares, P. Serras, I. Villaluenga, K. B. Hueso, J. Carretero-Gonzalez, T. Rojo, *Energy Environ. Sci.* **2012**, *5*, 5884.

[6] D. Aurbach, Z. Lu, A. Schechter, Y. Gofer, H. Gizbar, R. Turgeman, Y. Cohen, M. Moshkovich, E. Levi, *Nature* **2000**, *407*, 724.

[7] H. D. Yoo, I. Shterenberg, Y. Gofer, G. Gershinsky, N. Pour, D. Aurbach, *Energy Environ. Sci.* **2013**, *6*, 2265.

[8] M.-S. Park, J.-G. Kim, Y.-J. Kim, N.-S. Choi, J.-S. Kim, *Isr. J. Chem.* **2015**, *55*, 570.

[9] J. Muldoon, C. B. Bucur, T. Gregory, *Chem. Rev.* **2014**.

[10] M.-S. Park, J.-G. Kim, Y.-J. Kim, N.-S. Choi, J.-S. Kim, *Isr. J. Chem.* **2015**, *55*, 570.

[11] I. Shterenberg, M. Salama, Y. Gofer, E. Levi, D. Aurbach, *MRS Bull.* **2014**, *39*, 453.

[12] T. Mori, Y. Orikasa, K. Nakanishi, C. Kezheng, M. Hattori, T. Ohta, Y. Uchimoto, *J. Power Sources* **2016**, *313*, 9.

[13] Z. Yu, Z. Kang, Z. Hu, J. Lu, Z. Zhou, S. Jiao, *Chem. Commun.* **2016**, *52*, 10427.

[14] S. Wang, Z. Yu, J. Tu, J. Wang, D. Tian, Y. Liu, S. Jiao, *Adv. Energy Mater.* **2016**, *6*, 1600137.

[15] N. Jayaprakash, S. K. Das, L. A. Archer, *Chem. Commun.* **2011**, *47*, 12610.

[16] H. Wang, Y. Bai, S. Chen, X. Luo, C. Wu, F. Wu, J. Lu, K. Amine, *ACS Appl. Mater. Interfaces* **2015**, *7*, 80.

[17] S. Gu, H. Wang, C. Wu, Y. Bai, H. Li, F. Wu, *Energy Storage Mater.* **2017**, *6*, 9.

[18] M. Chiku, H. Takeda, S. Matsumura, E. Higuchi, H. Inoue, *ACS Appl. Mater. Interfaces* **2015**, *7*, 24385.

[19] W. Wang, B. Jiang, W. Xiong, H. Sun, Z. Lin, L. Hu, J. Tu, J. Hou, H. Zhu, S. Jiao, *Scientific Reports* **2013**, *3*, 3383.

[20] L. Geng, G. Lv, X. Xing, J. Guo, *Chem. Mater.* **2015**, *27*, 4926.

[21] M. P. Paranthaman, G. Brown, X.-G. Sun, J. Nanda, A. Manthiram, A. Manivannan, *Meeting Abstracts* **2010**, *MA2010-02*, 314.

[22] S. Wang, S. Jiao, J. Wang, H.-S. Chen, D. Tian, H. Lei, D.-N. Fang, *ACS Nano* **2017**, *11*, 469.

[23] G. Cohn, L. Ma, L. A. Archer, *J. Power Sources* **2015**, *283*, 416.

[24] N. P. Stadie, S. Wang, K. V. Kravchyk, M. V. Kovalenko, *ACS Nano* **2017**, *11*, 1911.

[25] M.-C. Lin, M. Gong, B. Lu, Y. Wu, D.-Y. Wang, M. Guan, M. Angell, C. Chen, J. Yang, B.-J. Hwang, H. Dai, *Nature* **2015**, *520*, 324.

[26] L. Tan, Y. Chi-lung, *Int. Geol. Rev.* **1970**, *12*, 778.

[27] T. Jiang, M. J. Chollier Brym, G. Dubé, A. Lasia, G. M. Brisard, *Surf. Coat. Tech.* **2006**, *201*, 10.

[28] T. Jiang, M. J. Chollier Brym, G. Dubé, A. Lasia, G. M. Brisard, *Surf. Coat. Tech.* **2006**, *201*, 1.

[29] J. J. Auborn, Y. L. Barberio, *J. Electrochem. Soc.* **1985**, *132*, 598.

[30] P. K. Lai, M. Skyllas-Kazacos, *J. Electroanal. Chem. Interfacial Electrochem.* **1988**, *248*, 431.

[31] J. Muldoon, C. B. Bucur, T. Gregory, *Chem. Rev.* **2014**, *114*, 11683.

[32] J. Liu, Y. Wan, W. Liu, Z. Ma, S. Ji, J. Wang, Y. Zhou, P. Hodgson, Y. Li, *J. Mater. Chem. A* **2013**, *1*, 1969.

[33] A. Eftekhari, P. Corrochano, *Sustainable Energy & Fuels* **2017**.

[34] S. Wang, K. V. Kravchyk, F. Krumeich, M. V. Kovalenko, *ACS Appl. Mater. Interfaces* **2017**, *9*, 28478.

[35] Y. Wu, M. Gong, M.-C. Lin, C. Yuan, M. Angell, L. Huang, D.-Y. Wang, X. Zhang, J. Yang, B.-J. Hwang, H. Dai, *Adv. Mater.* **2016**, *28*, 9218.

[36] X. Yu, B. Wang, D. Gong, Z. Xu, B. Lu, *Adv. Mater.* **2017**, *29*, 1604118.

[37] G. Y. Yang, L. Chen, P. Jiang, Z. Y. Guo, W. Wang, Z. P. Liu, *RSC Adv.* **2016**, *6*, 47655.

[38] S. C. Jung, Y.-J. Kang, D.-J. Yoo, J. W. Choi, Y.-K. Han, *J. Phys. Chem. C* **2016**, *120*, 13384.

[39] Y. Gao, C. Zhu, Z. Chen, G. Lu, *J. Phys. Chem. C* **2017**, *121*, 7131.

[40] X. Huang, Y. Liu, H. Zhang, J. Zhang, O. Noonan, C. Yu, *J. Mater. Chem. A* **2017**, DOI: 10.1039/C7TA04477A.

[41] J. V. Rani, V. Kanakaiah, T. Dadmal, M. S. Rao, S. Bhavanarushi, *J. Electrochem. Soc.* **2013**, *160*, A1781.

[42] K. V. Kravchyk, S. Wang, L. Piveteau, M. V. Kovalenko, *Chem. Mater.* **2017**, *29*, 4484.

[43] M. Angell, C.-J. Pan, Y. Rong, C. Yuan, M.-C. Lin, B.-J. Hwang, H. Dai, *Proc. Natl. Acad. Sci. U. S. A.* **2017**, *114*, 834.

[44] Y. Song, S. Jiao, J. Tu, J. Wang, Y. Liu, H. Jiao, X. Mao, Z. Guo, D. J. Fray, *J. Mater. Chem. A* **2017**, *5*, 1282.

[45] S. Jiao, H. Lei, J. Tu, J. Zhu, J. Wang, X. Mao, *Carbon* **2016**, *109*, 276.

[46] H. Sun, W. Wang, Z. Yu, Y. Yuan, S. Wang, S. Jiao, *Chem. Commun.* **2015**, *51*, 11892.

[47] P. Bhauriyal, A. Mahata, B. Pathak, *Phys. Chem. Chem. Phys.* **2017**, *19*, 7980.

[48] Z. Song, H. Zhou, *Energy Environ. Sci.* **2013**, *6*, 2280.

[49] K. C. Kim, *Ind. Eng. Chem. Res.* **2017**, *56*, 12009.

[50] S. Muench, A. Wild, C. Friebe, B. Häupler, T. Janoschka, U. S. Schubert, *Chem. Rev.* **2016**, *116*, 9438.

[51] T. Nokami, T. Matsuo, Y. Inatomi, N. Hojo, T. Tsukagoshi, H. Yoshizawa, A. Shimizu, H. Kuramoto, K. Komae, H. Tsuyama, J.-i. Yoshida, *J. Am. Chem. Soc.* **2012**, *134*, 19694.

[52] N. S. Hudak, *J. Phys. Chem. C* **2014**, *118*, 5203.

[53] J. C. Bachman, R. Kavian, D. J. Graham, D. Y. Kim, S. Noda, D. G. Nocera, Y. Shao-Horn, S. W. Lee, *Nat. Commun.* **2015**, *6*.

[54] S. C. Han, E. G. Bae, H. Lim, M. Pyo, *J. Power Sources* **2014**, *254*, 73.

[55] T. M. Figueira-Duarte, K. Müllen, *Chem. Rev.* **2011**, *111*, 7260.

[56] X.-G. Li , Y.-W. Liu, M.-R. Huang, S. Peng, L.-Z. Gong, M. G. Moloney, *Chem. - Eur. J.* **2010**, *16*, 4803.

[57] S. Califano, G. Abbondanza, *J. Chem. Phys.* **1963**, *39*, 1016.

[58] S. Zein El Abedin, *J Solid State Electrochem* **2012**, *16*, 775.

[59] J. M. Robertson, J. G. White, *J. Chem. Soc.* **1947**, 358.

[60] H. D. B. Jenkins, K. P. Thakur, *J. Chem. Educ.* **1979**, *56*, 576.

[61] E. Pretsch, P. Bühlmann, C. Affolter, E. Pretsch, P. Bhuhlmann, C. Affolter, *Structure determination of organic compounds*, Vol. 13, Springer, 2009.

[62] C. Wang, H. Dong, W. Hu, Y. Liu, D. Zhu, *Chem. Rev.* **2012**, *112*, 2208.

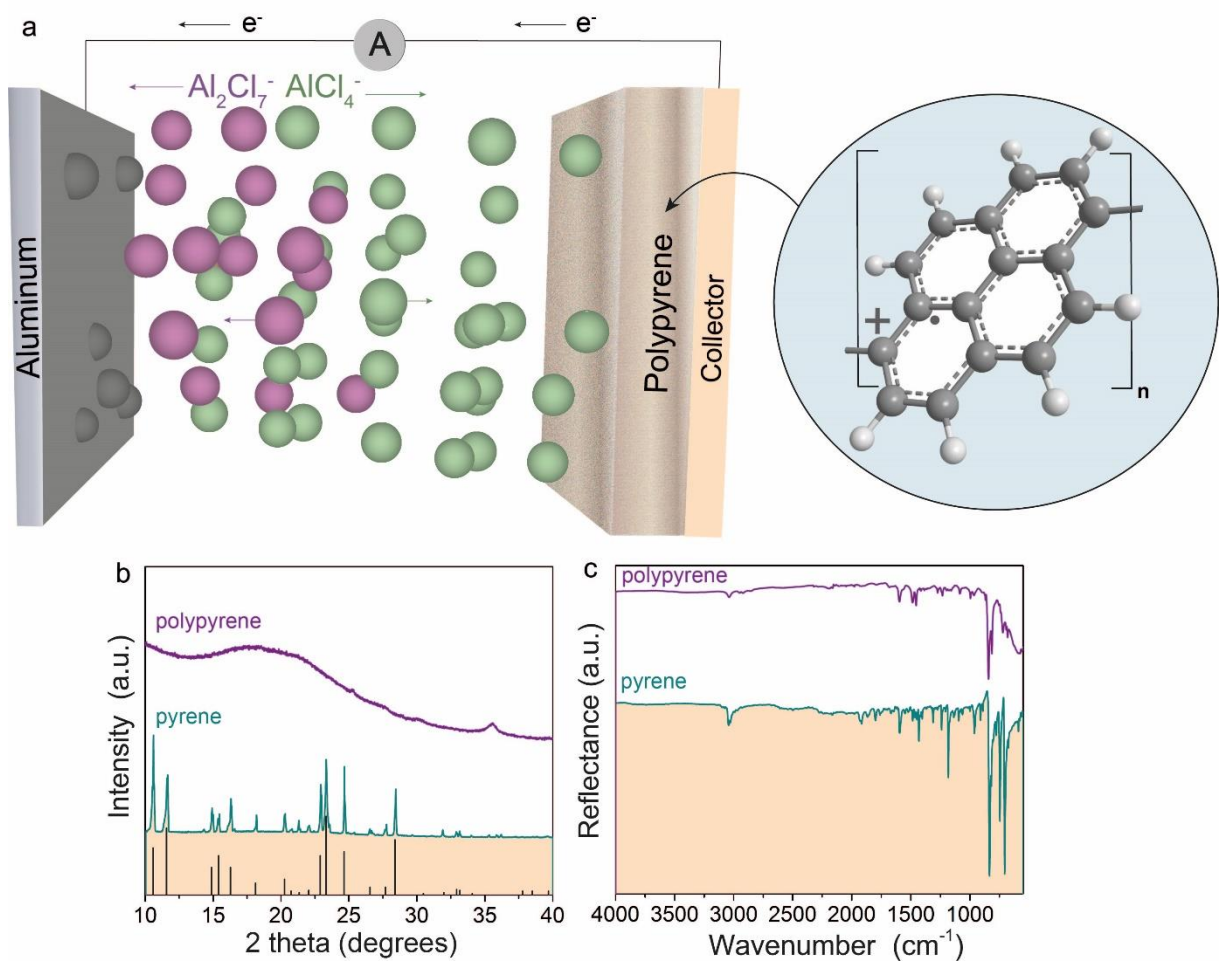

Figure 1. (a) Schematic of the working principle of a rechargeable aluminum battery during charge with a polypyrene cathode and chloroaluminate ionic liquid. (b) XRD pattern of crystalline pyrene (indexed to a known monoclinic polymorph; PDF entry No. 00-024-1855) and (c) FTIR-spectra of pyrene and polypyrene.

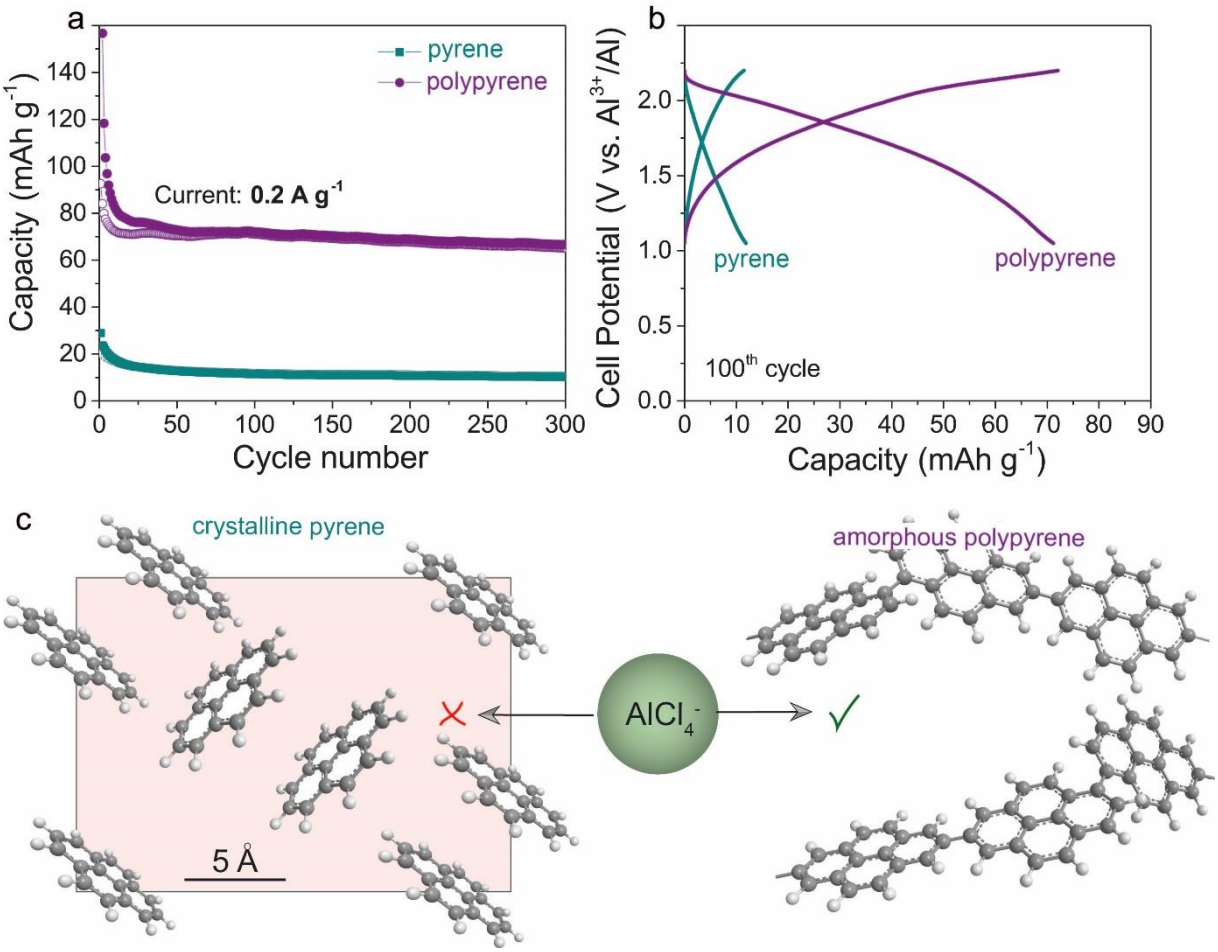

Figure 2. Electrochemical performance of aluminum batteries with pyrene and polypyrene as cathode materials: (a) capacity retention upon cycling and (b) corresponding charge/discharge voltage profiles for the 100th cycle. Cells were cycled at room temperature at a current density of 200 mA g^{-1} (referring to the mass of the polymer) in the potential range of 1.05–2.2 V. (c) Schematic representation of the structural differences between pyrene (crystalline, *e.g.,* dense molecular packing) and polypyrene (amorphous, porous and flexible), which impact their $AlCl_4^-$ storage behavior.

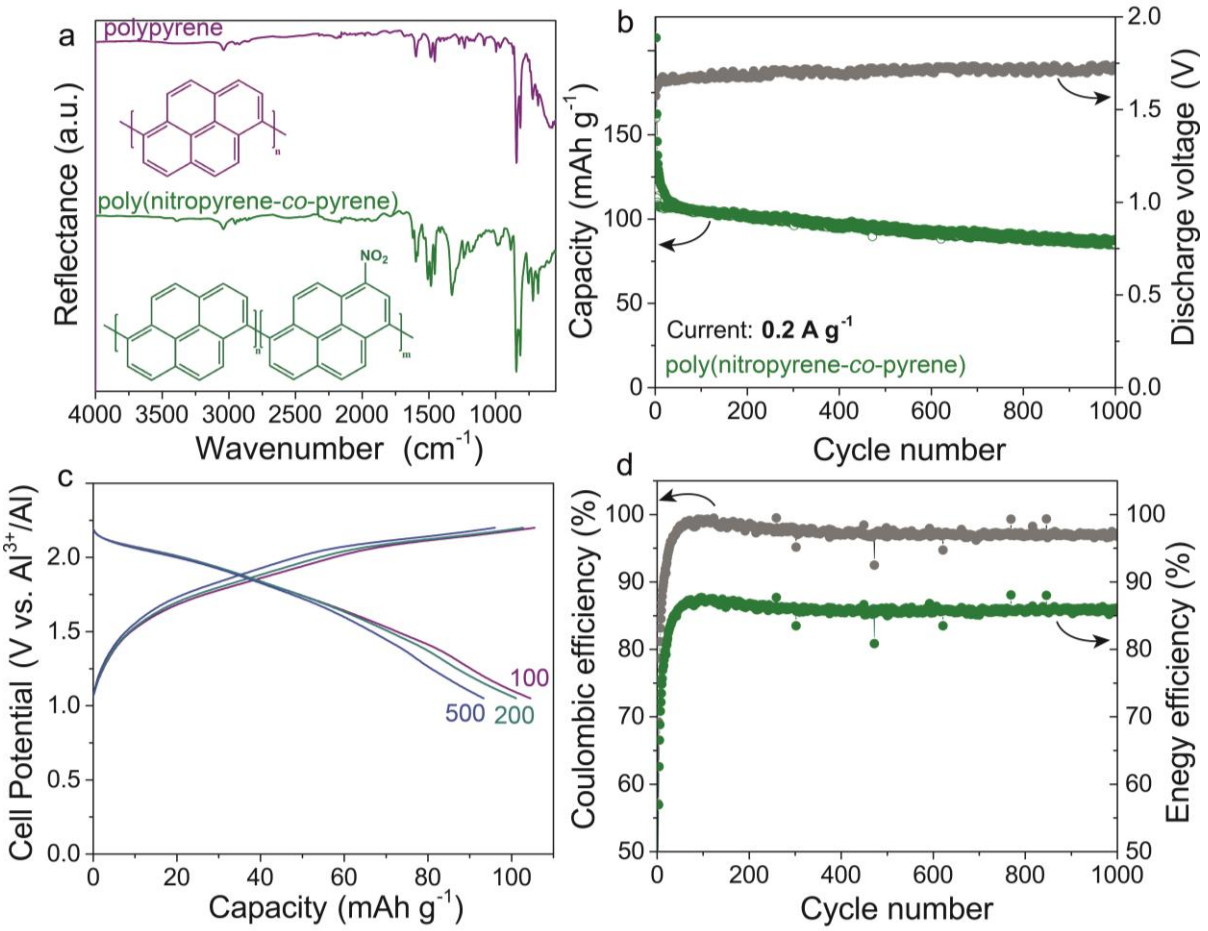

Figure 3. (a) FTIR-spectra of polypyrene (purple) and poly(nitropyrene-*co*-pyrene) (green). Electrochemical performance of aluminum batteries with poly(nitropyrene-*co*-pyrene) as the cathode material: (b) capacity retention upon cycling and average discharge voltages, (c) corresponding charge/discharge voltage curves for the 100th, 200th and 500th cycles and (d) coulombic and energy efficiencies. Cells were cycled at room temperature at a current density of 200 mA g^{-1} in the potential range of 1.05–2.2 V.

Pyrene-based polymers were demonstrated as high-performance cathode materials for aluminum batteries delivering capacities of up to 100 mAh g^{-1} at an average voltage of 1.7 V for at least 1000 cycles.

Keywords: Energy storage, aluminum batteries, pyrene, polypyrenes.

Marc Walter,[†,‡,#] Kostiantyn V. Kravchyk,[†,‡,#] Cornelia Böfer,[†,‡] Roland Widmer,[£] and Maksym V. Kovalenko[,†,‡]*

Polypyrenes as High-Performance Cathode Materials for Aluminum Batteries

ToC figure

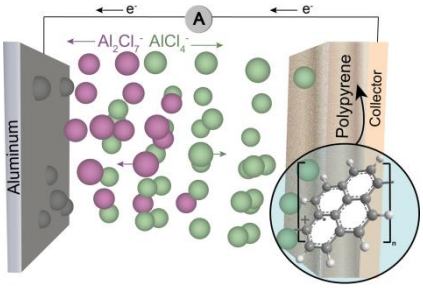

Supporting Information

Polypyrenes as High-Performance Cathode Materials for Aluminum Batteries

Marc Walter,[†,‡,#] *Kostiantyn V. Kravchyk,*[†,‡,#] *Cornelia Böfer,* [†,‡] *Roland Widmer,*[£] *and Maksym V. Kovalenko*[*,†,‡]

Calculation of theoretical gravimetric capacity of pyrene

Gravimetric capacity (C, in mAh g^{-1}) of an electrochemically active material can be calculated using the as follows:

$$C = \frac{x*F}{M} \qquad (1)$$

where $F = 26.8 \cdot 10^3$ mAh mol^{-1} (Faraday constant); x = number of electrons (in mols) used to oxidize/reduce 1 mol of the active material, M – molar mass of active material in g mol^{-1};

The theoretical capacity of pyrene is calculated based on a one-electron process per pyrene unit:

$$C = \frac{1*F}{202.25} \approx 133 \text{ mAh } g^{-1} \qquad (2)$$

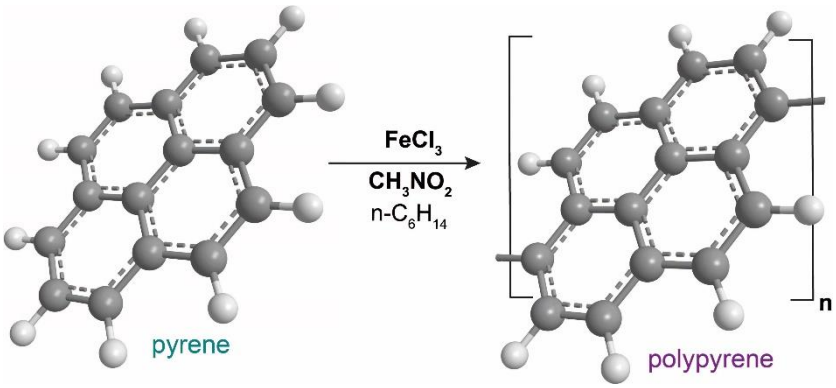

Figure S1. Reaction scheme for the synthesis of polypyrene according to Li *et al*.[1]

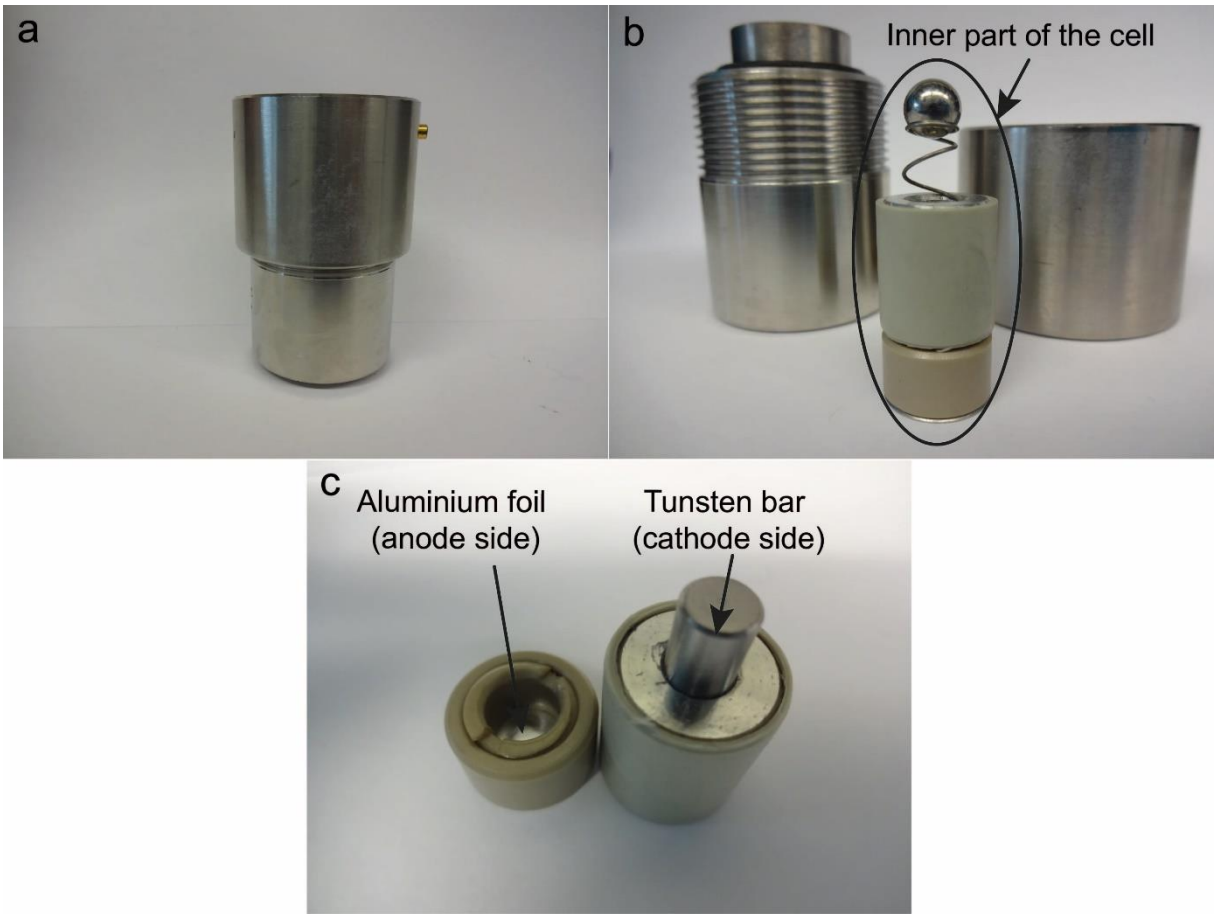

Figure S2. Custom-made cell used for electrochemical measurements.

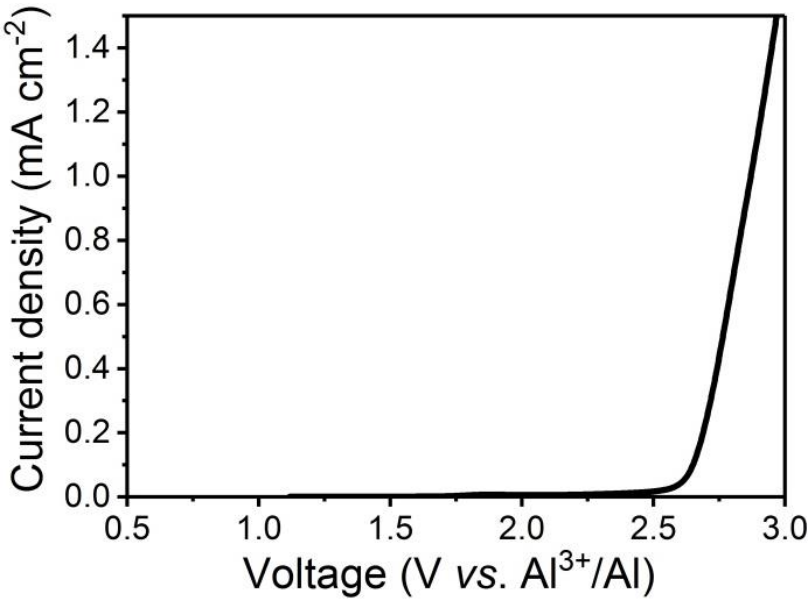

Figure S3. Cyclic voltammetry curve for tungsten current collector measured in $AlCl_3$-[EMIm]Cl ionic liquid (2:1 mol. ratio) at a rate of 10 mV s^{-1}.

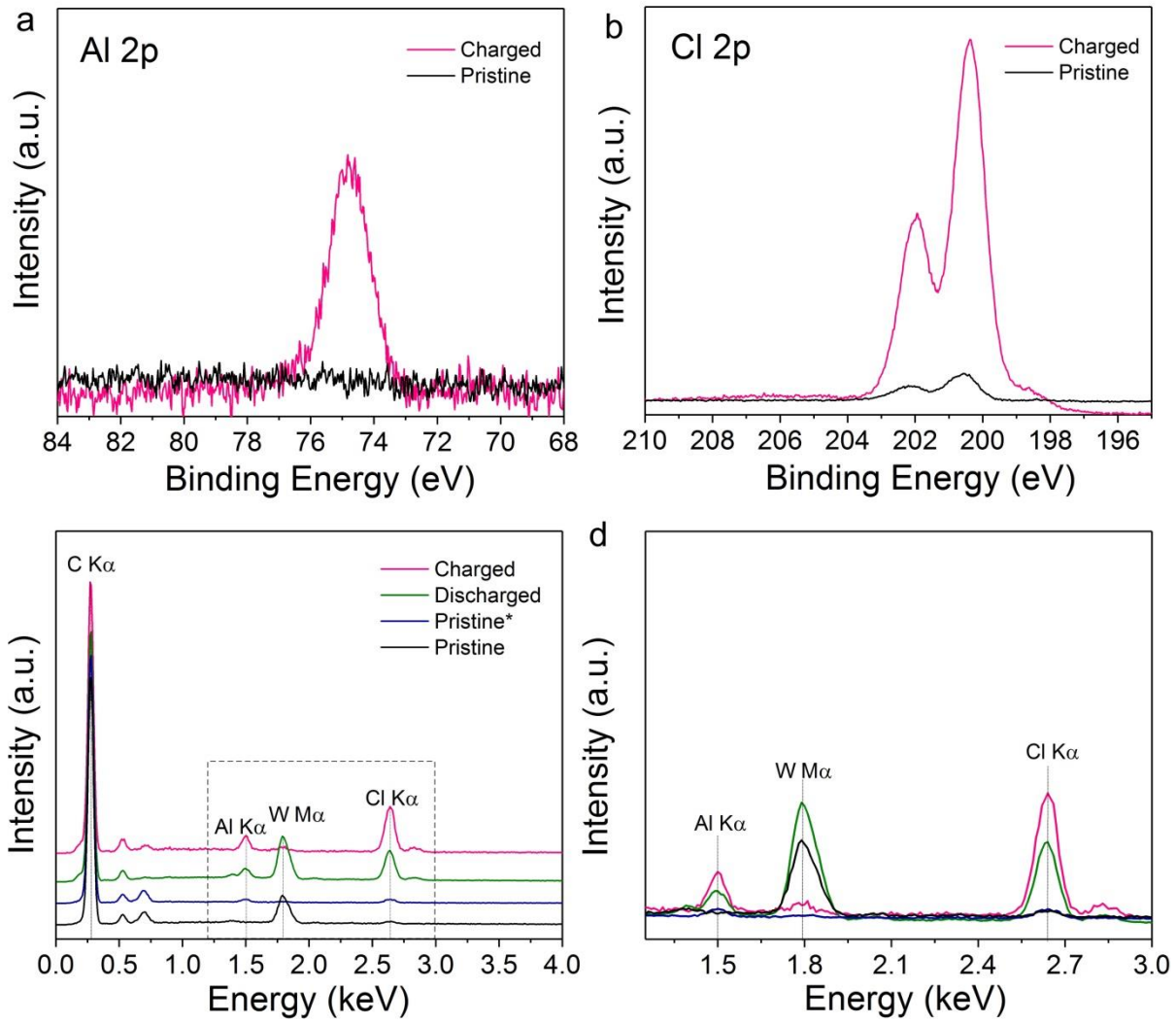

Figure S4. Detail XP spectra of (a) Al 2p and (b) Cl 2p of charged and pristine polypyrene electrodes. (c, d) EDX spectra of charged, discharged, pristine* and pristine electrodes (figure d shows comparison of intensities of Al Kα and Cl Kα peaks normalized by the intensity of C Kα peak). Charged and discharged electrodes were prepared by electrochemical charging or discharging of polypyrene electrodes at current density of 200 mA g^{-1} (2^{nd} cycle), followed by washing with anhydrous acetonitrile (ACN) as an oxidatively stable solvent capable of removing the ionic liquid. Sample designated as Pristine* was prepared by impregnation of polypyrene electrode in $AlCl_3$:EMIMCl electrolyte, followed by washing with ACN. Small intensity of Al Kα and Cl Kα peaks after the washing procedure for Pristine* sample confirms removal of chloroaluminate ionic liquid from the surface of polypyrene electrode. The remaining Al Kα and Cl Kα peaks for discharged sample can be attributed to the trapped $AlCl_4^-$ ions after the first charge.

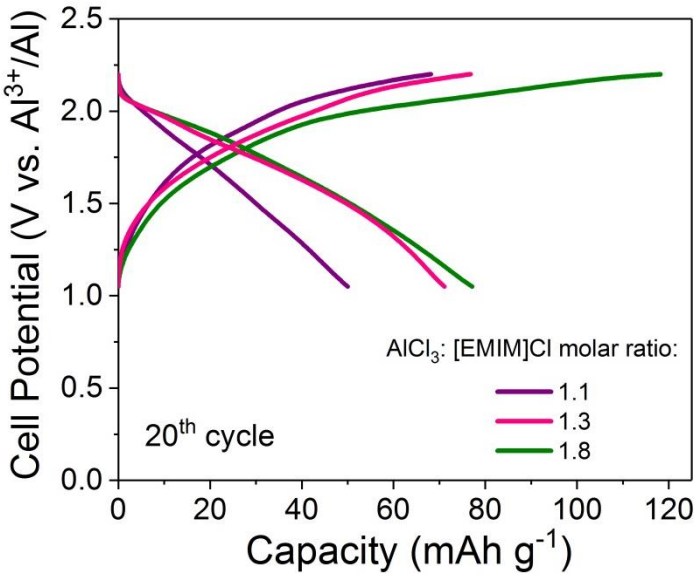

Figure S5. Charge/discharge voltage profiles for the 20th cycle of a polypyrene cathode at various molar ratios of $AlCl_3$:EMIMCl ionic liquid (1.1, 1.3, 1.8). Cells were cycled at room temperature at a current density of 200 mA g^{-1} (referring to the mass of the polymer) in the potential range of 1.05–2.2 V.

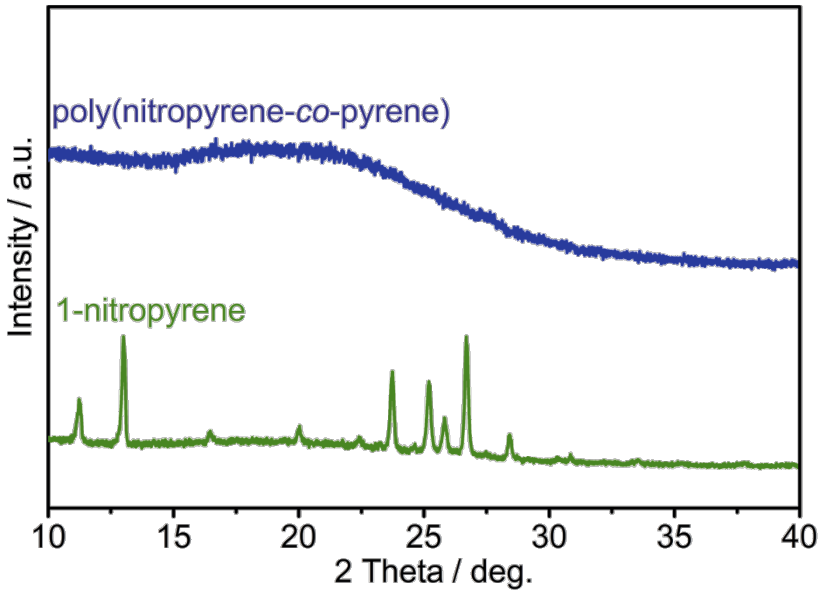

Figure S6. Comparison of the XRD patterns of poly(nitropyrene-*co*-pyrene) and 1-nitropyrene).

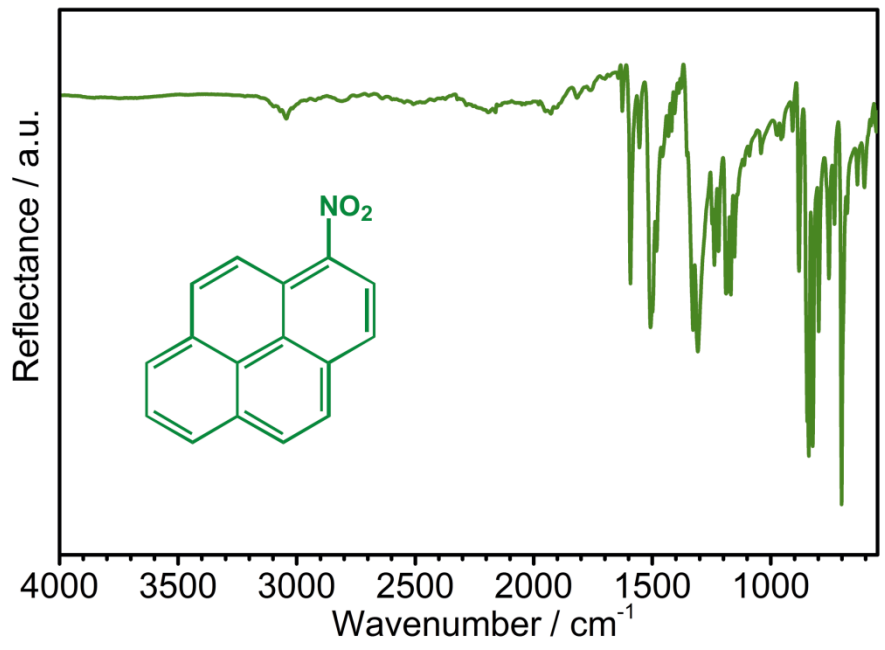

Figure S7. FTIR-spectrum of 1-nitropyrene.

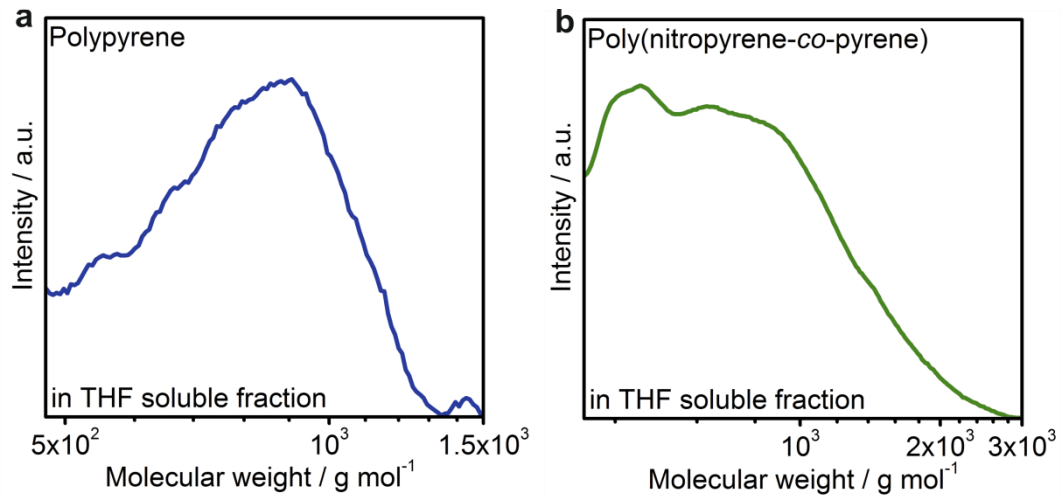

Figure S8. Gel permeation chromatography in THF soluble fractions of (a) polypyrene and (b) poly(nitropyrene-*co*-pyrene).

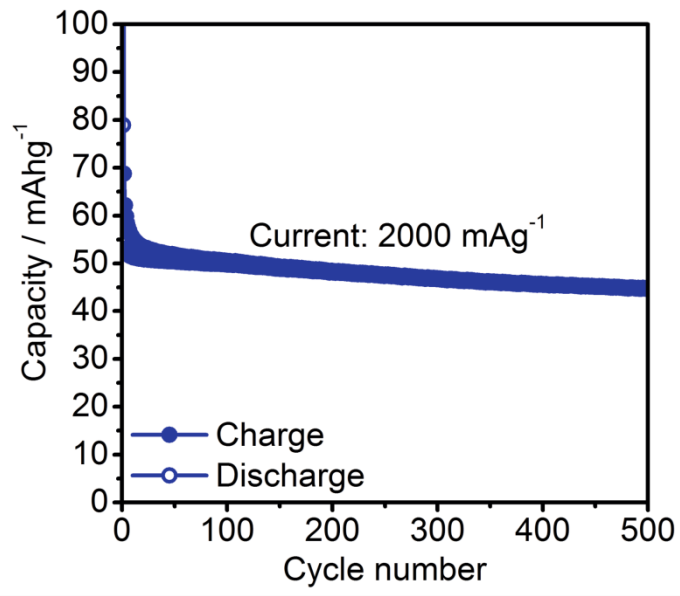

Figure S9. Capacity retention of poly(nitropyrene-*co*-pyrene) as cathode material in aluminum battery. Cells were cycled at room temperature with a current density of 2000 mA g^{-1} in the potential range of 1.05–2.2 V.

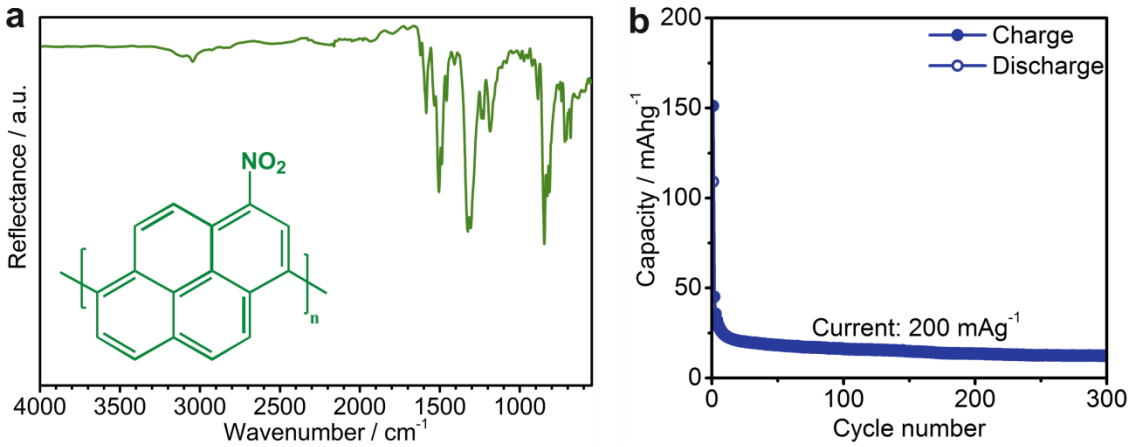

Figure S10. (a) FTIR-spectrum and (b) capacity retention for polynitropyrene prepared using the same conditions as for polypyrene and poly(nitropyrene-*co*-pyrene) with only 1-nitropyrene as starting material. Cells were cycled at room temperature with a current density of 200 mA g^{-1} in the potential range of 1.05–2.2 V.

Table S1. Comparison of the electrochemical performance of the herein presented polypyrene and with other polymeric materials reported as cathode materials for aluminum batteries.

Cathode material	Current density	Average capacity	Cycle number	Average discharge voltage
Poly(nitropyrene-*co*-pyrene)	200 mA g^{-1}	100 mAh g^{-1}	500	~1.7 V
(present work)		94 mAh g^{-1}	1000	~1.7 V
Polypyrrole[2]	20 mA g^{-1}	~55 mAh g^{-1}	100	~1.2 V
Polythiophene[2]	16 mA g^{-1}	~75 mAh g^{-1}	100	~1.4 V

References

1. X.-G. Li , Y.-W. Liu, M.-R. Huang, S. Peng, L.-Z. Gong and M. G. Moloney, *Chem. - Eur. J.*, 2010, **16**, 4803-4813.
2. N. S. Hudak, *J. Phys. Chem. C*, 2014, **118**, 5203-5215.